Chinese Journal of Chemical Engineering 56 (2023) 290–298

Contents lists available at ScienceDirect

Chinese Journal of Chemical Engineering

journal homepage: www.elsevier.com/locate/CJChE

Full Length Article

Nanoparticle-induced drag reduction for polyacrylamide in turbulent flow with high Reynolds numbers

Xiaoping Li [1], Jiaxin Pan [1], Jinwen Shi [1,*], Yanlin Chai [1], Songwei Hu [1], Qiaorong Han [2], Yanming Zhang [2], Xianwen Li [2], Dengwei Jing [1,*]

[1] State Key Laboratory of Multiphase Flow in Power Engineering & International Research Center for Renewable Energy, Xi'an Jiaotong University, Xi'an 710049, China
[2] Oil and Gas Technology Research Institute of Petrochina Changqing Oilfield Company, Xi'an 710018, China

ARTICLE INFO

Article history:
Received 9 March 2022
Received in revised form 6 July 2022
Accepted 15 July 2022
Available online 22 July 2022

Keywords:
Drag reduction
SiO_2 nanoparticle
Cationic polymer
Brownian motion

ABSTRACT

Although having been increasingly studied, there is still controversy as to when the addition of nanoparticles could improve the drag reduction performance of polymer drag reducer and particularly what is the underlying mechanism from the fluid dynamics viewpoint. The drag reduction effects of adding SiO_2 nanoparticles to various polymer polyacrylamide (PAM) solutions were examined in this work. The optimal combination of SiO_2 nanoparticles with cationic polyacrylamide was confirmed. Interestingly, the addition of SiO_2 nanoparticles to cationic polyacrylamide solution was shown to be quite efficient for reducing drag, but only at higher flow rates with Reynolds numbers more than 6000, below which the nanoparticle addition is even negative. The addition of SiO_2 nanoparticles to the PAM solution is supposed to play a dual role. The first is an increase in flow resistance caused by the Brownian motion of nanoparticles, while the second is a decrease in flow resistance caused by acting as nodes to protect the polymer chain from shear-induced breaking under high shear action. At optimal nanoparticle concentration and under higher Reynolds numbers, the later effect is dominant, which could improve the drag reduction performance of polymer drag reducers. Our work should serve as a guide for the application of natural gas fracturing, where the flow rate is frequently very high.

1. Introduction

When drag reducer like polymer, surfactant, fibers, *etc.*, is added, a lower pressure drop might be acquired for the fluid, thus increasing piping system capacity and reducing pumping power [1–6]. As the most widely used drag reducer in industry areas, the polymer can cause a drag reduction effect at very low concentrations, the synergism in drag reduction by the polymer-fiber mixtures also was observed [7–9]. However, when suffering high shear rates, polymer molecular chains would break and lose their drag reduction properties. Moreover, the mechanical breakdown of polymer chains is permanent and cannot recover when shear action disappears [10–13]. Yang and Ding [14] dealt with the velocity distribution and friction factor of polymer drag reducing flows in smooth pipes and discussed the effect of polymer mechanical degradation. They considered that the mechanical degradation of polymer chains leads to the alternation of molecular weight. Zhang *et al.* [15] developed a new method to predict the friction factor in pipe flow applicable to a wide range of pipe diameters. They found that the slope and intercept of these straight lines could be predicted by empirical correlations involving diameters and polymer concentrations. The physical meanings of the slope and intercept were pointed out and made it clear why the previous scaling law became not reliable when it was employed to predict the friction factor for pipe flow with a too wide range of pipe diameters.

Studies have shown that adding surfactant into the polymer solution can increase the drag reduction performance on account of the formation of an assembly and improve the resistance of molecular chains against shear failure [16–19]. Gu *et al.* [20] discussed the factors affecting the degradation of polymer additives and the anti-degradation properties of surfactants. It was found that the mixture of polymer additive and surfactant had the characteristics of high shear resistance, a lower critical micelle concentration (CMC), and a good drag reduction effect at higher Reynolds numbers. In recent years, nanoparticles and surfactants have been used to reduce the surface tension of fracturing fluid [21–26], and change the wettability of fracturing fluid and formation rock

* Corresponding authors.
E-mail addresses: jinwen_shi@mail.xjtu.edu.cn (J. Shi), dwjing@xjtu.edu.cn (D. Jing).

https://doi.org/10.1016/j.cjche.2022.07.015
1004-9541/

[27–30]. Steele *et al.* [31] investigated the drag reduction effects of dispersing carbon nanotube (CNT) additives into the water–glycerin pipe flow. The results showed that CNTs could enhance the drag-reducing characteristics of polymer additives. Interestingly, the CNTs by themselves do not provide drag reduction in the turbulent regime and their additive benefit is lost once the polymers degrade.

However, there exists great controversy on whether the addition of nanoparticles can improve the drag reduction performance of the original drag reducer or not [32]. Rosti and Brandt [33] studied the effect of spherical particles on the turbulent flow of viscoelastic fluid and found that the drag-reducing effect of polymer additives was completely lost for suspensions, with the drag increasing more than for suspensions in Newtonian fluids. However, more researchers believe that the small-scale effect and Brownian effect of nanoparticles cause the disordered movement of surfactant micelles, which increases the flow resistance [16,34–36]. And others consider that nanoparticles can act as the cross-linking agent between surfactant micelles, and promote the surfactant assembling into a three-dimensional network structure, then the viscoelasticity will be enhanced, and the ability to reduce flow resistance will be improved [37]. Some reported that nanoparticles added in surfactant solution will deposit on the inner wall of the pipe as the fluid flows, which can reduce the roughness of the pipe, thus reducing the flow resistance [38]. It is considered that the surface of nanoparticles can interact with the end cap of linear micelles, acting as a bond, and connecting the micelles into a micelle network [39].

There are some reports about the effect of nanoparticles on the rheological properties and drag reduction properties of polymer solutions [40,41]. It has been reported that when nanoparticles are added to polymer drag reducing fluid, the stretched polymer molecular chain will lose its original regular shape, thus increasing the flow resistance [36]. Although the viscosity of the base solution increases with the addition of nanoparticles, the effects on the drag reduction performance are quite different: the addition of polymer reduces the pressure drop, while nanoparticles increase the pressure drop. Sharma *et al.* [42] studied the viscosity of the mixed SiO_2 nanoparticle polyacrylamide (PAM) solution and found that the viscosity of the mixed solution of SiO_2 nanoparticle and PAM was higher than that of the PAM solution alone. They believed that a complex molecular structure was formed due to the interaction between SiO_2 nanoparticles and PAM. Xing *et al.* [43] developed a novel nanocomposite drag reducer (PASD-SiO_2) modifying nanosilica by redox free-radical copolymerization. The efficiency of maximum drag reduction for PASD-3% SiO_2 was found to be 59.2%, 9.7% higher than neat polymer. There is still controversy over when the addition of nanoparticles could improve the drag reduction performance of polymer drag reducers and particularly what the underlying mechanism is.

In this work, we studied the drag reduction characteristics when SiO_2 nanoparticles were added to PAM solution of different charges, trying to find out the optimal combinations. We have paid particular attention to the conditions under which the addition of nanoparticles could improve the drag reduction performance of polymer drag reducers and what the underlying mechanism is. This work should be valuable for the design of new drag reduction systems for applications such as natural gas fracturing and transport of fluids.

2. Materials and Methods

2.1. Materials

The PAM is the main representative of polymer drag reduction and has been widely used in the oilfield fracturing process. In addition, compared the drag reduction performance of polyethylene oxide (PEO), PAM, and xanthan gum (XG) polymers, PAM performed the best [44], which is the reason why we chose PAM. Three kinds of PAM, *i.e.*, cationic PAM, anionic PAM, and nonionic PAM with a molecular weight of $M_v = 1.6 \times 10^7$, were used. Its overlap concentration is 511 $mg \cdot L^{-1}$, by measuring the intrinsic viscosity of the PAM solution and then calculating the overlap concentration [45]. The base fluid used in this work was tap water with a conductivity of around 216 $\mu S \cdot cm^{-1}$. Commercial hydrophilic SiO_2 nanoparticles with sizes ranging between 7–40 nm (specific surface area, ~380 $m^2 \cdot g^{-1}$) were employed. All reagents mentioned above were of analytical grade, and purchased from Aladdin Industry Co. (Shanghai, China).

2.2. Sample preparation

Typically, the nanoparticles and polymers were dissolved in tap water, respectively. Then, they were mixed in the tank under constant stirring. Here, nanoparticle suspensions were prepared by dispersing a certain amount of nanoparticles into tap water. The ultra-sonication treatment with frequency and amplitude of 30 kHz and 60% was applied for 30 min to disperse powders in the suspensions. In another procedure, PAM was added to tap water and kept stationary for 12 h at room temperature. The polymer solution was then subjected to full stirring at 500 $r \cdot min^{-1}$ for about 2 h at (40 ± 0.5) °C until a homogenous solution is obtained.

2.3. Experimental setup and measurement methods

The experiment was carried out in a closed-loop system as shown in Fig. 1 that we had set up in our previous work [17]. A screw pump pushed the solution mixed in the tank into the pipe loop. The test section of the pipe was stainless steel tube with an inner diameter of 8 mm. The temperature of the solution in the test section was maintained at (20 ± 0.5)°C by the water bath out of the pipe. A flowmeter and a differential pressure transmitter were used to monitor the flow rate and pressure drop of the test portion, respectively. The measuring accuracy was 0.01 $m^3 \cdot h^{-1}$ and 0.1 kPa, respectively. And an energy accumulator was used to ensure that the flow rate and pressure in the test section were relatively stable between the experiments. The drag reduction experiment starts by making the system run smoothly at a certain flow rate so that both the solution as well as the system reach a steady state. Afterward, the liquid flow rate through the test section is changed by continuously adjusting the flow regulating valve, and when the flow rate reaches a stable level, the pressure sensor is recorded and the experiment is repeated continuously so that the flow rate is cycled from low to high three times. The three steady-state pressure values under each flow rate are recorded, and the three pressure values are averaged to be the experimental pressure drop under the flow rate. Therefore, the steady-state pressure value after three measurements is the steady-state value.

The size and morphology of the nanoparticles were determined on a transmission electron microscope (TEM, Tecnai G2 F30 S-TWIN, FEI, USA). For this measurement, the liquid sample was dripped onto a Cu grid with carbon coating and then dried at room temperature. The zeta potential of the sample was investigated using a Zetasizer Nano-ZS90 apparatus (Malvern, UK). The pH value was measured using a Five Easy Plus FE28-S pH meter (Mettler, Switzerland).

2.4. Data processing

Relevant studies [46] have shown that PAM solutions have a straight rheological curve at very low concentrations, exhibit the properties of a Newtonian fluid, and have a fixed viscosity. There-

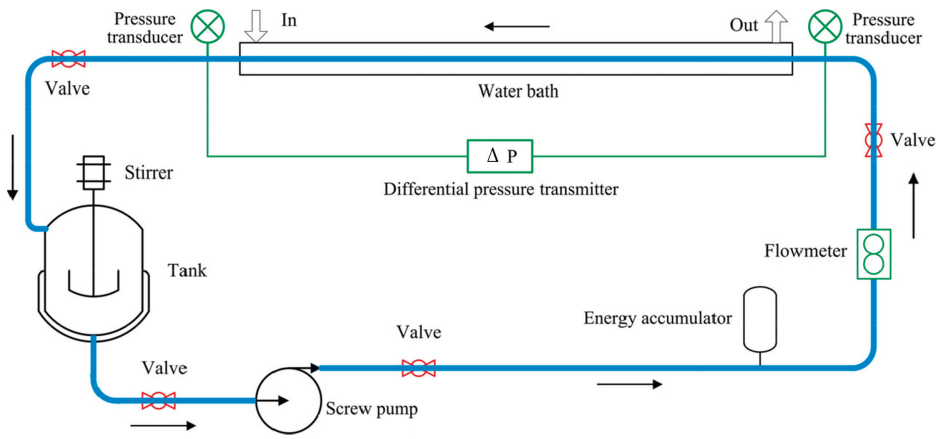

Fig. 1. Diagram of experiment system.

fore, the Reynolds number (*Re*) is determined as follows in this work:

$$Re = \frac{\rho u d}{\mu} \tag{1}$$

where ρ, u, d, and μ are the density of the solution, the mean velocity of the solution, the inner diameter of the test pipeline, and the dynamic viscosity of the solution, respectively.

The effectiveness of drag reduction is determined by the percentage of drag reduction (DR, %) in solution which is usually expressed quantitatively as follows:

$$\mathrm{DR} = \frac{\Delta P_{\text{without additives}} - \Delta P_{\text{with additives}}}{\Delta P_{\text{without additives}}} \times 100\% \tag{2}$$

where $\Delta P_{\text{without additives}}$ is the pressure drop of solution without additives and $\Delta P_{\text{with additives}}$ is the pressure drop of solution with additives.

3. Results and Discussion

3.1. Characterization of nanoparticles

It is known that similar kinds of nanoparticles may have different hydrophilicity and hydrophobicity due to different surface microstructures. The surface properties of the nanoparticles can also be changed by functionalization. Generally, one should select the appropriate surface responsive particles according to the intended application. Therefore, it is necessary to determine the characteristics of nanoparticles according to the charge and surface properties of selected polymers.

3.1.1. Size analysis of nanoparticles

Fig. 2 shows the TEM images of SiO_2 nanoparticles in suspensions. The result shows that the shape of nanoparticles is nearly spherical. The average size of primary particles is determined to be 10–20 nm. Irregular shapes of large bundles are also shown in Fig. 2, which suggests the obvious aggregation of nanoparticles. As is known, the specific surface area and surface energy of nanoparticles are large. When dispersed in the liquid phase, they will spontaneously agglomerate to reduce the surface energy until the agglomerated particles reach a balance size. Then the particles will be in a dynamic equilibrium state of agglomeration and fragmentation, but the average size of particles will not change obviously.

3.1.2. Surface properties of nanoparticles

To ensure the full dispersion of SiO_2 nanoparticles in water, hydrophilic SiO_2 nanoparticles were considered in the present experiment. The contact angle between the SiO_2 nanoparticle dispersion solution and the glass sheet was measured and the result is shown in Fig. 3. It can be found in Fig. 3 that the contact angle between the SiO_2 nanoparticle dispersion solution and the glass sheet is nearly zero. Therefore, we can conclude that the nanoparticles used in the experiment are very hydrophilic.

3.1.3. Zeta potential of nanoparticles

When SiO_2 nanoparticles are dispersed in the solution, the ions on the surface of the particles will dissociate or absorb other ions, thus making the surface of the particles charged. What's more, the interaction between nanoparticles and polymer chains depending on the electric property of the nanoparticle surface and particle

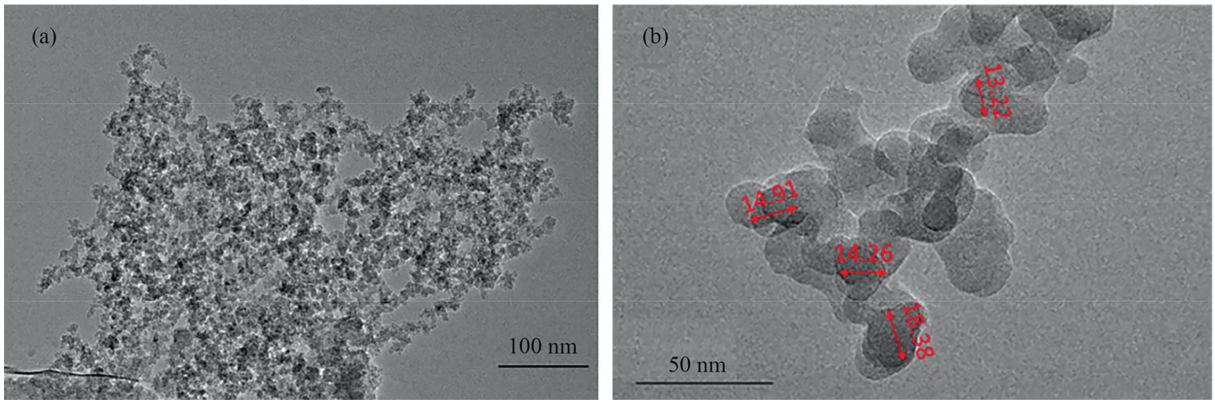

Fig. 2. TEM images of SiO_2 nanoparticles.

Fig. 3. Contact angle of SiO_2 nanoparticles dispersion solution.

size has a great influence on the drag reduction behavior. To determine the surface electrical properties of the particles, the zeta potential of SiO_2 nanoparticle suspensions at different pH values was determined. As shown in Fig. 4, the zeta potential of SiO_2 nanoparticle suspensions decreases with the increase of pH value. When the zeta potential is zero, the corresponding pH value is about 2.1. The zeta potential will be positive when the pH value is less than 2.1 and the zeta potential will be negative when it is greater than 2.1. Therefore, we can conclude that the surface of SiO_2 nanoparticles is negatively charged under neutral conditions.

3.2. Drag reduction effect of SiO_2 nanoparticles with different kinds of PAM

The interaction between negatively charged SiO_2 nanoparticles and PAM with different ionic characteristics may show different drag reduction performances. To study the interaction between SiO_2 nanoparticles and different kinds of polyacrylamide, here in our study, the concentrations of SiO_2 and PAM were selected to be 5000 and 100 $mg{\cdot}L^{-1}$, respectively [47] (the concentration of SiO_2 and PAM were in mass concentration units). Then the drag reduction behaviors of SiO_2 nanoparticles with three different kinds of PAM, *i.e.*, cationic, anionic, and nonionic, have been investigated, respectively. Fig. 5 shows the drag reduction effect of different combinations at a certain flow rate. All of the experiments are repeated three times to ensure accuracy. It should be noted that the interaction between zwitterionic PAM and SiO_2 nanoparticles will be more complex for the special characteristics of both the anionic group and cationic group, thus the zwitterionic PAM was not considered in our present study.

As shown in Fig. 5, the drag reduction rate shows a gradual downward trend with the increase of Reynolds number for pure

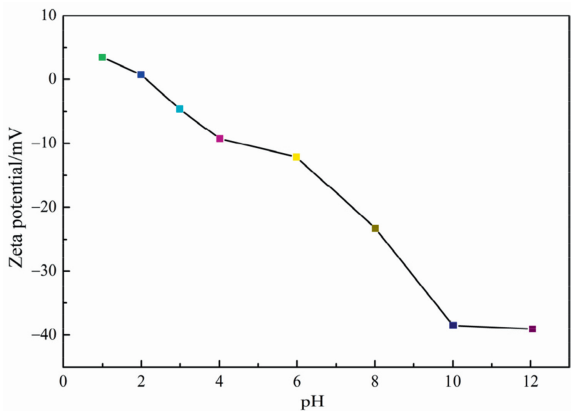

Fig. 4. Zeta potential of SiO_2 nanoparticles suspension.

100 $mg{\cdot}L^{-1}$ PAM solution. When the Reynolds number exceeds 7000, the drag reduction rate decreases to almost zero, and the drag reduction performance is significantly reduced. We believe that the fracture of polymer molecules chains at a high shear rate resulted in the disability of drag reduction [48,49], which is consistent with our previous investigation [17].

For the mixture of SiO_2 nanoparticles and PAM, the trend of drag reduction rate increases with the increase of the Reynolds number. The drag reduction rate of the mixture of SiO_2 nanoparticles and cationic PAM increases more obviously with the increase of the Reynolds number. At a low Reynolds number, it is assumed that the small-scale effect and obvious Brownian motion of nanoparticles cause the disordered movement of fluid microclusters in the flow field [50]. The smaller the Reynolds number is, the more obvious the effect will be. With the increase of Reynolds number, the velocity of fluid micro cluster increases, and the disturbance of flow field caused by the disordered movement of nanoparticles will be weakened, then the drag reduction rate increases gradually under the action of the PAM molecular chain.

For the drag reduction curve of pure PAM and the mixture system of SiO_2 nanoparticles and PAM, at a low Reynolds number (less than 6000), the drag reduction performance of pure PAM solution is better than the mixture system. That is to say, in such a case, the addition of nanoparticles has a negative impact on the drag reduction performance of PAM. It is believed that the disordered movement of the fluid micro cluster in the flow field resulted from a small-scale effect and the obvious Brownian motion effect of nanoparticles disturbs the original flow field [50]. Meanwhile, the electrostatic interaction between nanoparticles and polymer molecular chains may cause the molecular chain of polyacrylamide to be curled, thus weakening the drag reduction ability. At a high Reynolds number (more than 7000), the drag reduction performance of the mixture system is better than that of a pure PAM solution. Obviously, the addition of nanoparticles has a positive impact on the drag reduction performance of PAM in this case. It is supposed that, with the increase of Reynolds number, the shear effect gradually increases. The crimped PAM molecular chain caused by the electrostatic and hydrophobic effect of nanoparticles gradually expands under the shear action, and the nanoparticles will act as a junction point to protect the PAM molecular chain from fracturing, so that at high Reynolds number SiO_2 nanoparticles and PAM mixture system can maintain strong drag reduction performance. The addition of nanoparticles can solve the problem of polymer molecular chain fracture and the loss of drag reduction ability under high shear rates, which can provide some guidance for the use of polymers as drag-reducing additives in systems with high flow and shear rates.

In order to find the difference in drag reduction performance when nanoparticles were combined with differently charged PAM, we further studied PAM of cationic, anionic, and non-ionic properties, respectively, under the same concentration of 100 $mg{\cdot}L^{-1}$. The nanoparticle concentration was kept to 5000 $mg{\cdot}L^{-1}$. The drag reduction fraction under certain flow rates of 0.35, 0.40, 0.45, and 0.50 $m^3{\cdot}h^{-1}$, were investigated. The drag reduction performance of anionic PAM, cationic PAM, and nonionic PAM mixture systems is shown in Fig. 6.

As shown in Fig. 6, when the flow rate is lower, the drag reduction fractions over three different charged mixture systems are all negative. That is to say, the addition of nanoparticles will be detrimental to the drag reduction performance of PAM and increase the flow resistance. As mentioned above, at a low flow rate, for the lower movement rate of fluid micro clusters and weaker shear action, the addition of nanoparticles causes PAM molecular chains to intertwine, thus weakening their drag reduction property. On the contrary, the disordered Brownian motion of nanoparticles will lead to an increase in flow resistance. In conclusion, when the flow

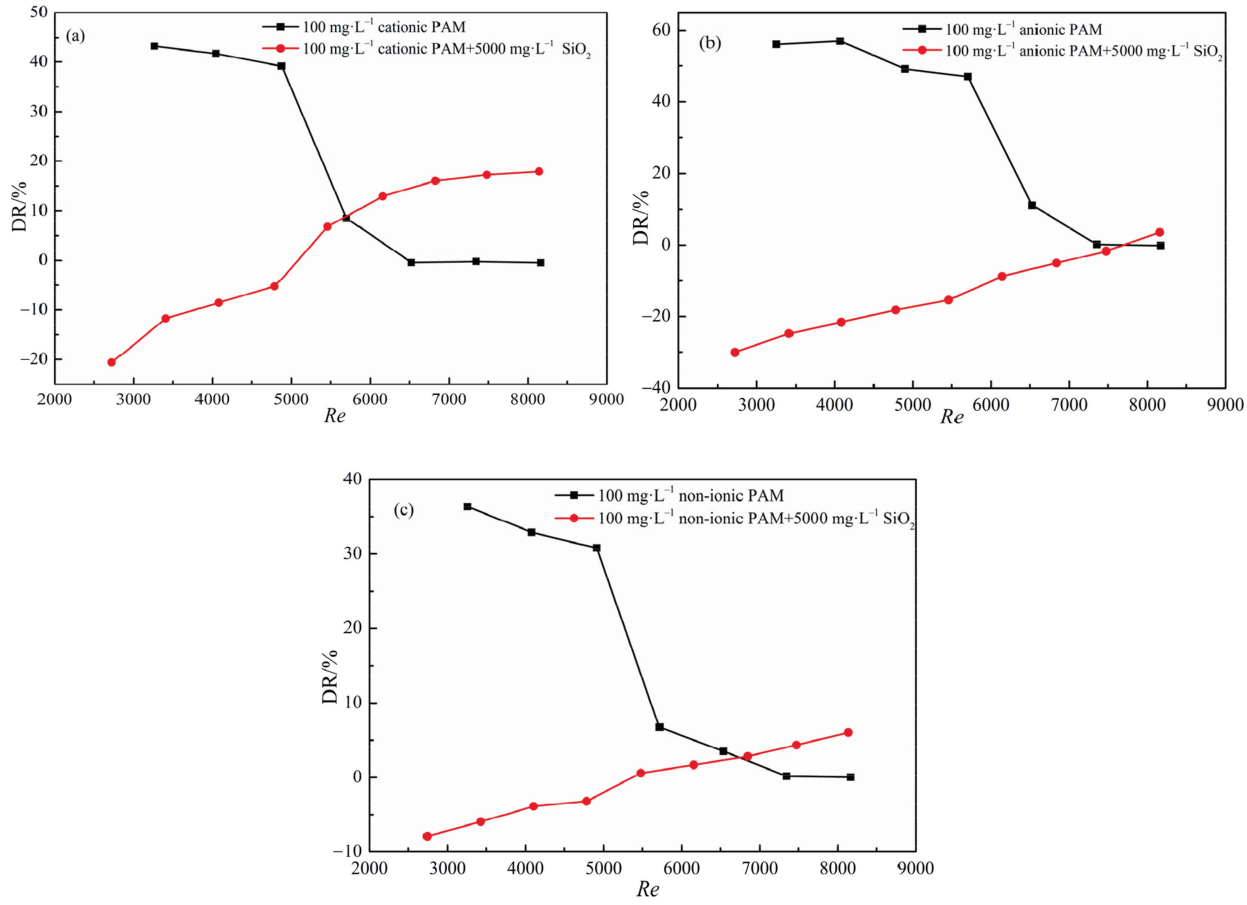

Fig. 5. Drag reduction behavior of different kinds of PAM induced by SiO_2 nanoparticles: (a) cationic PAM, (b) anionic PAM, (c) non-ionic PAM.

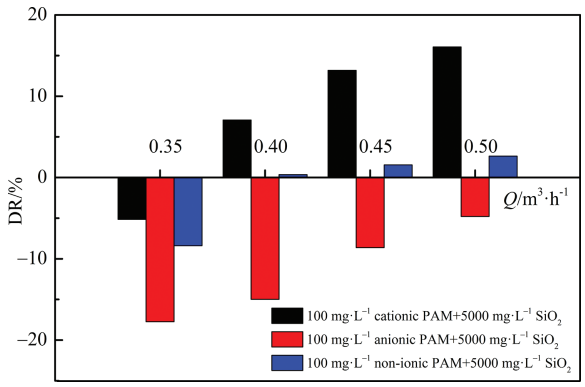

Fig. 6. Drag reduction rate of different charged PAM systems induced by SiO_2 nanoparticles, as a function of flow rate.

rate is lower, the addition of nanoparticles has a negative effect on the drag reduction performance of PAM with different charges.

Interestingly, as the flow rate increases, the effect of nanoparticles addition on the drag reduction performance of cationic PAM and non-ionic PAM will change from the negative effect of increasing flow resistance to the positive effect of reducing flow resistance. With the increase in flow rate furthermore, the positive effect will be more and more evident. Meanwhile, the effect of nanoparticles addition on the drag reduction of cationic PAM is better than that of non-ionic PAM at a high flow rate. However, for anionic PAM, the addition of nanoparticles leads to the increasing flow resistance of the system in our tested range. The different interaction between nanoparticles and PAM mainly depends on the electrostatic interaction between the negatively charged nanoparticles and PAM with different charges. We assume that the strong electrostatic repulsion between the same charged anionic PAM and nanoparticles facilitates the PAM molecules chain to be completely outstretched. The drag reduction performance of the outstretched polymer chain will be better, but the elasticity weaker. When the shear rate increases further, polymer chains with lower elasticity are liable to breakdown, then the performance of drag reduction will decrease rapidly [51].

On the other hand, the disordered Brownian motion of the nanoparticles leads to the rising of flow resistance. For non-ionic PAM, the electrostatic interaction is rather weaker, and the disordered Brownian motion of particles at a low flow rate leads to an increase in flow resistance. While at a high flow rate, the nanoparticles may act as the nodes between polymer molecular chains to protect the polymer molecular chain from breaking under shear action, then the expanding PAM chain will maintain preferable drag reduction performance. Significantly, for cationic PAM, the molecular chains intertwine together at low flow rates due to the strong electrostatic attraction between opposite charged nanoparticles and PAM, which is not desired for drag reduction. With the increase of flow rate, the molecular chains of polymer will expand gradually under the shear action, then the drag reduction performance restore. As mentioned, nanoparticles can also act as nodes. In addition, the negative effect of increasing flow resistance caused by the Brownian motion of nanoparticles will be weakened with respect to the intense turbulence flow field. Therefore, the combination of nanoparticles and cationic PAM showed the best drag reduction performance at a high flow rate.

3.3. Effect of nanoparticle concentration on drag reduction behavior of cationic PAM

As analyzed above, the addition of SiO_2 nanoparticles plays a dual role. On the one hand, the disordered turbulent flow field of Brownian motion increases the flow resistance. On the other hand, nanoparticles acting as nodes between PAM molecular chains can protect the molecular chains from breaking under a high shear rate. When the negative effect is stronger, the addition of nanoparticles will increase the flow resistance. When the positive effect prevails, the addition of nanoparticles will reduce the flow resistance.

The effect of nanoparticles addition on drag reduction performance of PAM is not only related to the charge of PAM but also affected by the concentration of nanoparticles. In order to further study the effect of nanoparticle concentration on the drag reduction performance of PAM, we selected the best combination of nanoparticles and cationic PAM achieved in the above experiments, and chose the concentration of nanoparticles as 2500, 5000, 7500, and 10000 mg·L^{-1}, respectively, to investigate the drag reduction behavior. The results are shown in Fig. 7.

The drag reduction curves of the mixed solution of four concentrations, *i.e.*, 2500, 5000, 7500, and 10000 mg·L^{-1}, are shown in Fig. 7(a) to (d), respectively. The results indicate that the performance of drag reduction of mixed solution is different from that of pure PAM solution. But the four curves show the same trend: with the increase of Reynolds number, the impact of nanoparticles on drag reduction performance of cationic PAM presents a transition from negative impact to positive impact. The difference in drag reduction performance is more evident at a higher Reynolds number. The drag reduction data of mixed solution with different nanoparticles concentrations at high flow rates (higher than 0.3 m^3·h^{-1}) are shown in Fig. 8, in order to present the drag reduction phenomenon under a higher shear rate in our experiment evidently.

It can be found clearly from Fig. 8 that the mixed solution with 5000 mg·L^{-1} nanoparticles shows better drag reduction behavior. To be specific, for the 5000 mg·L^{-1} nanoparticle mixture, the negative effect of increasing flow resistance is the lowest compared with other concentrations when the flow rate is 0.35 m^3·h^{-1}, and the positive effect of reducing flow resistance is the best compared with other concentrations when the flow rate is more than 0.35 m^3·h^{-1}. In other words, when the concentration of nanoparticles is 5000 mg·L^{-1}, the interaction between nanoparticles and cationic PAM can protect the PAM molecular chain from fracturing at a high flow rate, thus maintaining a higher drag reduction rate. As mentioned above, the addition of nanoparticles to cationic PAM shows a dual effect. Similarly, when the concentration of nanoparticles is higher, the negative effect and the positive effect both exist. It is speculated that when the nanoparticle concentration is 5000 mg·L^{-1}, the negative effect of increasing flow resistance caused by Brownian motion is relatively small, and the nanoparticles in the system are enough to prevent PAM molecular chain from breaking under high shear. Once the concentration exceeds 5000 mg·L^{-1}, the extra nanoparticles will not have a stronger protective effect on PAM molecular chain, but increase the flow resistance due to the Brownian motion. Therefore, when the concentration of nanoparticles is 5000 mg·L^{-1}, the best drag reduction effect is achieved.

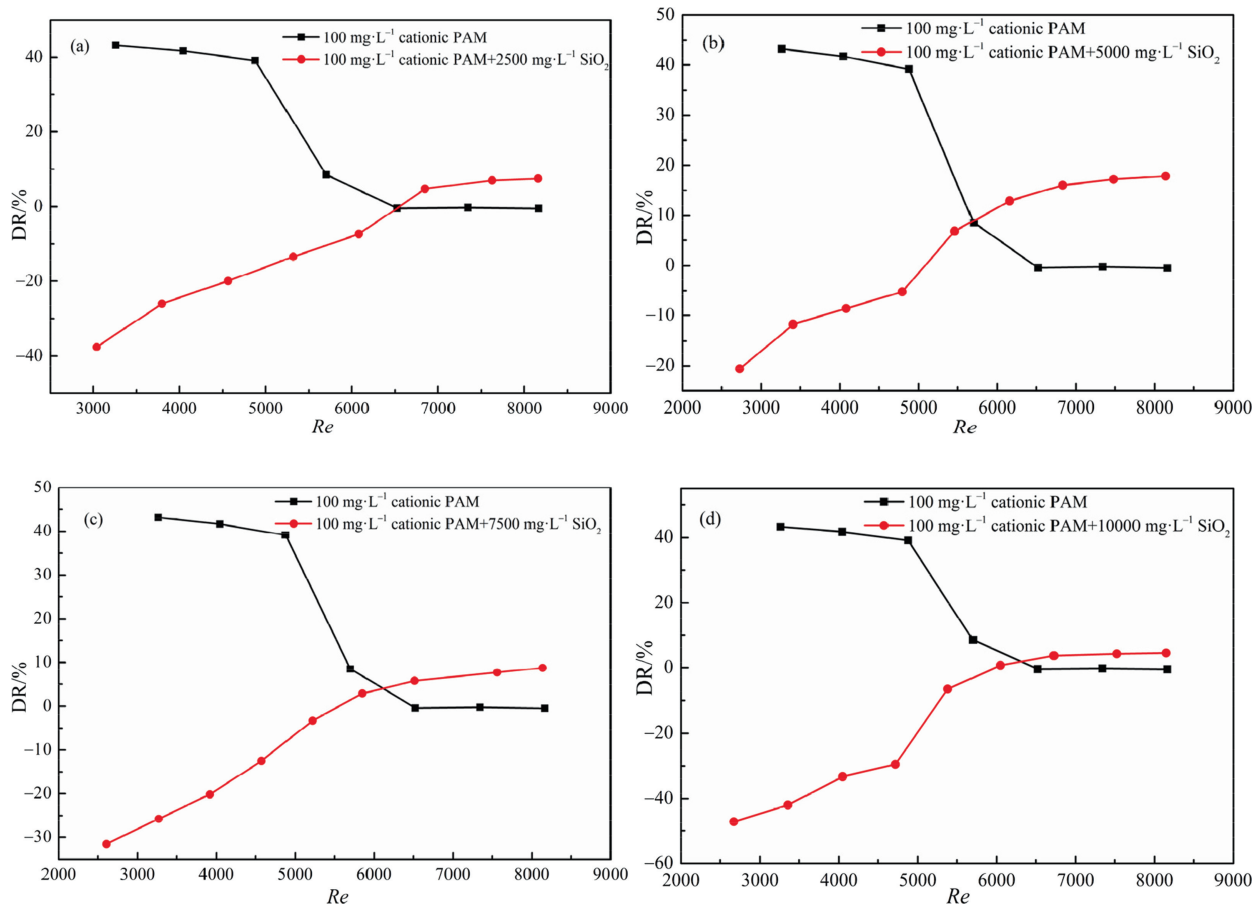

Fig. 7. Drag reduction behavior of cationic PAM induced by SiO_2 nanoparticles, as a function of nanoparticles concentration.

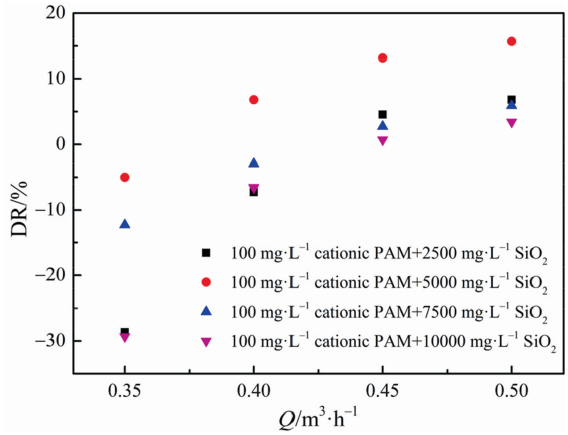

Fig. 8. Drag reduction behavior of mixed solution at a high flow rate (higher than 0.3 $m^3 \cdot h^{-1}$).

3.4. Mechanism discussion

The probable illustration of the interaction of PAM with 5000 $mg \cdot L^{-1}$ nanoparticle under different shear rates (with the flow rates lower and higher than 0.35 $m^3 \cdot h^{-1}$) is shown schematically in Fig. 9 to illustrate the interaction of PAM molecular chain and nanoparticle, as well as the change of the structure of the assembly.

As shown in Fig. 9, when 5000 $mg \cdot L^{-1}$ nanoparticle is added to cationic PAM solution, the electrostatic attraction between nanoparticles and cationic PAM results in the curing of the molecular chain of PAM leading to the significantly lowered drag reduction ability under lower shear action. Simultaneously, the Brownian motion of nanoparticles will disturb the normal flow field and increase the flow resistance. Under high shear rates, the molecular chain curled due to the electrostatic attraction will gradually expand and the nanoparticles will then act as nodes between polymer molecules. The nodes between the chains can protect the polymer molecules from shear fracture and maintain preferable drag reduction ability.

There are many explanations and models for polymer drag reduction, but few theories can be employed to explain all the experimental phenomena in the turbulent flow such as in our present case. The popular hypotheses are Toms pseudo plastic hypothesis, effective slip hypothesis, turbulence pulsation suppression hypothesis, turbulence pulsation decoupling hypothesis, and viscoelasticity hypothesis [52,53]. Up to now, the viscoelastic hypothesis is widely accepted, which holds that the polymer molecules have viscoelasticity and play an important role in drag reduction. Due to the interaction between viscoelasticity and turbulent vortex, part of the energy in the vortex will be absorbed by the drag reducer molecules, and stored in the way of elastic energy. By reducing the vortex flow energy, the drag reduction effect can be achieved.

For viscoelastic fluid, the practical shear stress formula can be obtained from the Maxwell model:

$$\tau = \mu D \frac{\mathrm{d}\bar{u}}{\mathrm{d}y} \tag{3}$$

where the drag-reduction parameter D is defined as follows:

$$D = 1 + C\alpha_0[\eta]\frac{\pi^2}{15}e^{\left(-2.55\times10^4\alpha_0^{0.7}C_w\right)}Re^* \tag{4}$$

Here, τ is the shear stress of the fluid at the discussion point, $N \cdot m^{-2}$; μ is the dynamic viscosity coefficient of the fluid, Pa·s; α_0 is the polymer performance parameter; C is polymer concentration; Re^* is the friction Reynolds number; C_w is polymer concentration by mass and $[\eta]$ is intrinsic viscosity coefficient of the polymer.

According to the expression of drag reduction parameter D, we infer that the drag reduction effect of polymer is directly proportional to the concentration C, and the larger the molecular weight of the polymer, the better the drag reduction effect will be. It can be seen from the formula that the larger the drag reduction parameter D is, the greater the shear force that the polymer molecule can bear. Therefore, it can be considered that when SiO_2 nanoparticles are added to cationic PAM, the electrostatic interaction between nanoparticles and PAM molecular chain facilitates the nanoparticle's role as the nodes between polymer molecular chains under higher shear action. It can increase the length of the molecular chain, which is equivalent to increasing the molecular weight of the polymer, thus increasing the drag reduction parameter D of the polymer and the shear resistance ability.

For the drag reduction reaction point of dilute polymer solution, the following relationship was concluded by Virk [54]:

$$R_G\left(\tau_w^*\right)^{1/2} = D_f \tag{5}$$

where R_G is the mean square radius of gyration of the macromolecule, τ_w^* is the critical wall shear stress of drag reduction reaction point, and D_f is physical property constant depending on drag reduction agent.

The formula above shows that drag reduction can only occur when the product of R_G representing the size of micelle and its shear stress exceeds the C value. Therefore, for the mixture system of SiO_2 nanoparticles and cationic PAM, the radius of rotation of micelles, the shear stress, and the physical property constant of

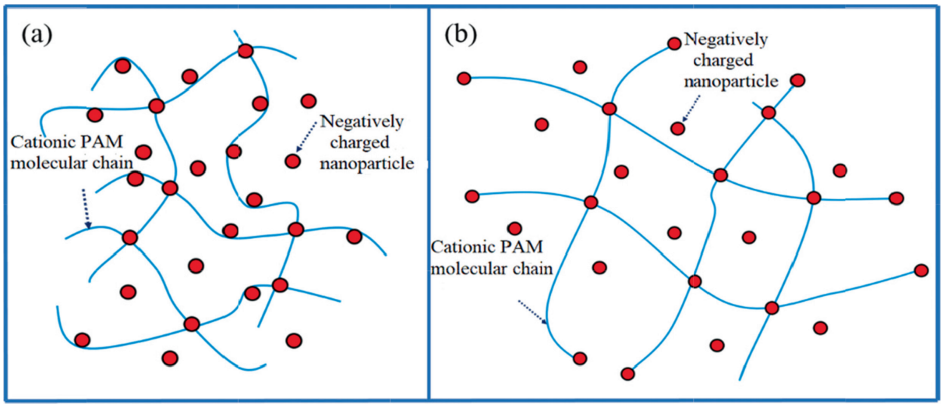

Fig. 9. Illustration of the interaction of PAM with 5000 $mg \cdot L^{-1}$ nanoparticle under (a) low and (b) high shear rate.

the drag reducer all increase with the increase of shear rate. Therefore, at a high Reynolds number, the addition of SiO_2 nanoparticles will protect the cationic PAM molecular chain from shear fracture and maintain a certain drag reduction performance, in agreement with the previous analysis.

4. Conclusions

In this work, we studied the drag reduction characteristics when SiO_2 nanoparticle was added to PAM solution of different charges, trying to find out the optimal combinations. We have paid particular attention to what condition under which the addition of nanoparticles could improve the drag reduction performance of polymer drag reducer and what is the underlying mechanism. The main outcomes of our study are summarized as below:

(1) At a low Reynolds number of less than 6000, the Brownian motion of nanoparticles causes the disordered movement of the fluid microcluster. Meanwhile, the electrostatic interaction between nanoparticles and polymer molecules causes the polymer chain to curl, which increases the flow resistance of the flow.
(2) At a high Reynolds number more than 6000, the curled polymer chain gradually extends under high shear rates. Moreover, nanoparticles acting as the nodes among molecular chains can prevent the PAM chain from breaking, which can maintain preferable drag reduction performance. While the Brownian motion effect of nanoparticles is insignificant at a high flow rate.
(3) The optimal drag reduction performance is obtained for the SiO_2 nanoparticle concentration of around 5000 $mg{\cdot}L^{-1}$. SiO_2 nanoparticles added in cationic PAM solution were supposed to play a dual role. One is increasing flow resistance resulting from the Brownian motion of nanoparticles and the other is reducing flow resistance with nanoparticles acting as nodes due to the electrostatic attraction of opposite charges to protect the molecular chain from shear-induced breaking under high shear action. When the concentration of nanoparticles is around 5000 $mg{\cdot}L^{-1}$, the later effect is dominant and one can acquire the best drag reduction performance under a high shear rate.

CRediT Authorship Contribution Statement

Xiaoping Li: Conceptualization, Software, Writing – original draft, Formal analysis, Validation, Visualization. **Jiaxin Pan:** Formal analysis, Writing – review & editing, Supervision. **Jinwen Shi:** Formal analysis, Writing – review & editing. **Yanlin Chai:** Conceptualization, Software, Writing – original draft. **Songwei Hu:** Formal analysis, Writing – review & editing. **Qiaorong Han:** Formal analysis. **Yanming Zhang:** Formal analysis. **Xianwen Li:** Formal analysis. **Dengwei Jing:** Conceptualization, Writing – review & editing, Supervision.

Data Availability

Data will be made available on request.

Declaration of Competing Interest

The authors declare that they have no known competing financial interests or personal relationships that could have appeared to influence the work reported in this paper.

Acknowledgements

The authors gratefully acknowledge the financial supports of the National Natural Science Foundation of China (51961130386) the National Science Fund for Distinguished Young Scholars (52025061). This work was also supported by the China Fundamental Research Funds for the Central Universities.

References

[1] R. Benzi, E.S.C. Ching, Polymers in fluid flows, *Annu. Rev. Conden. Ma. P.* 9 (2018) 163–181.
[2] B. Yang, J.Z. Zhao, J.C. Mao, H.Z. Tan, Y. Zhang, Z.F. Song, Review of friction reducers used in slickwater fracturing fluids for shale gas reservoirs, *J. Nat. Gas Sci. Eng.* 62 (2019) 302–313.
[3] E.J. Soares, Review of mechanical degradation and de-aggregation of drag reducing polymers in turbulent flows, *J. Non Newton. Fluid Mech.* 276 (2020) 104225.
[4] A.M. Fsadni, J.P.M. Whitty, M.A. Stables, A brief review on frictional pressure drop reduction studies for laminar and turbulent flow in helically coiled tubes, *Appl. Therm. Eng.* 109 (2016) 334–343.
[5] L.X. Cheng, D. Mewes, A. Luke, Boiling phenomena with surfactants and polymeric additives: A state-of-the-art review, *Int. J. Heat Mass Transf.* 50 (13–14) (2007) 2744–2771.
[6] M.M. Wu, G.G. Shi, W.M. Liu, Y.F. Long, P. Mu, J. Li, A universal strategy for the preparation of dual superlyophobic surfaces in oil–water systems, *ACS Appl. Mater. Interfaces* 13 (12) (2021) 14759–14767.
[7] G.V. Reddy, R.P. Singh, Drag reduction effectiveness and shear stability of polymer-polymer and polymer-fibre mixtures in recirculatory turbulent flow of water, *Rheol. Acta* 24 (3) (1985) 296–311.
[8] A. Eshghinejadfard, K. Sharma, D. Thévenin, Effect of polymer and fiber additives on pressure drop in a rectangular channel, *J. Hydrodyn. Ser. B* 29 (5) (2017) 871–878.
[9] C. Marchioli, M. Campolo, Drag reduction in turbulent flows by polymer and fiber additives, *KONA Powder Part. J.* 38 (2021) 64–81.
[10] H. Chen, H.Z. Liu, S. Zhang, Y.J. Feng, Smart thermoviscosifying polymer for improving drag reduction in slick-water hydrofracking, *Fuel* 278 (2020) 118408.
[11] H.J. Shashank, K.R. Sreenivas, Effect of polymer solutions on the propagation and structure of freely translating vortex rings, *Chem. Eng. Sci.* 228 (2020) 115961.
[12] A.D.N. Celestine, V. Agrawal, B. Runnels, Experimental and numerical investigation into mechanical degradation of polymers, *Compos. B Eng.* 201 (2020) 108369.
[13] W.L. Lai, H. Saeedipour, K.L. Goh, Mechanical properties of low-velocity impact damaged carbon fibre reinforced polymer laminates: Effects of drilling holes for resin-injection repair, *Compos. Struct.* 235 (2020) 111806.
[14] S.Q. Yang, D.H. Ding, Drag reduction induced by polymer in turbulent pipe flows, *Chem. Eng. Sci.* 102 (2013) 200–208.
[15] X. Zhang, X.D. Dai, J.S. Zhao, D.W. Jing, F. Liu, L. Li, Y.P. Xin, K. Liu, Precise prediction of the drag reduction efficiency of polymer in turbulent flow considering diameter effect, *Phys. Fluids* 33 (9) (2021) 095124.
[16] S.S. Alsaedi, Z.Y. Shnain, M.K. Rashed, P. Filip, Triple solutions of nanoparticle plus polymer-surfactant compound for enhancing the drag reduction using a rotational disk apparatus, *IOP Conf. Ser.: Mater. Sci. Eng.* 881 (1) (2020) 012079.
[17] Y.L. Chai, X.W. Li, J.F. Geng, J.X. Pan, Y.L. Huang, D.W. Jing, Mechanistic study of drag reduction in turbulent pipeline flow over anionic polymer and surfactant mixtures, *Colloid Polym. Sci.* 297 (7–8) (2019) 1025–1035.
[18] J.T. Jiang, X. Kang, H.R. Wu, Y. Lu, Z. Li, D.R. Xu, T. Ma, H.B. Yang, W.L. Kang, Spontaneous emulsification induced by a novel surfactant-polymer compound system and its application to enhance oil recovery, *J. Mol. Liq.* 337 (2021) 116399.
[19] E. Weißenborn, J. Droste, M. Hardt, D. Schlattmann, C. Tennagen, C. Honnigfort, M. Schönhoff, M.R. Hansen, B. Braunschweig, Light-induced switching of polymer-surfactant interactions enables controlled polymer thermoresponsive behaviour, *Chem. Commun.* 57 (47) (2021) 5826–5829.
[20] Y.Q. Gu, S.W. Yu, J.G. Mou, D.H. Wu, S.H. Zheng, Research progress on the collaborative drag reduction effect of polymers and surfactants, *Materials (Basel)* 13 (2) (2020) 444.
[21] K.Q. Zhang, N. Jia, S.Y. Li, L.R. Liu, How surfactant-decorated nanoparticles contribute to thermodynamic miscibility, *Nanotechnology* 29 (47) (2018) 475701.
[22] J.Y. Jin, X.Y. Li, J.F. Geng, D.W. Jing, Insights into the complex interaction between hydrophilic nanoparticles and ionic surfactants at the liquid/air interface, *Phys. Chem. Chem. Phys.* 20 (22) (2018) 15223–15235.
[23] Q.W. Tang, Z.Y. Huang, B.G. Wang, H.S. Lu, Surfactant-free aqueous foams stabilized with synergy of xanthan-based amphiphilic biopolymer and nanoparticle as potential hydraulic fracturing fluids, *Colloids Surf. A Physicochem. Eng. Aspects* 603 (2020) 125215.
[24] T. Lin, H.X. Wang, H.M. Wang, X.G. Wang, The charge effect of cationic surfactants on the elimination of fibre beads in the electrospinning of polystyrene, *Nanotechnology* 15 (9) (2004) 1375–1381.

[25] H. Divandari, A. Hemmati-Sarapardeh, M. Schaffie, M. Ranjbar, Integrating functionalized magnetite nanoparticles with low salinity water and surfactant solution: Interfacial tension study, *Fuel* 281 (2020) 118641.
[26] M. Latikka, M. Backholm, A. Baidya, A. Ballesio, A. Serve, G. Beaune, J.V.I. Timonen, T. Pradeep, R.H.A. Ras, Ferrofluid microdroplet splitting for population-based microfluidics and interfacial tensiometry, *Adv. Sci.* 7 (14) (2020) 2000359.
[27] Y.L. Wang, J.F. Jin, L. Ma, L. Li, X. Zhao, Influence of wettability alteration to preferential gas-wetting on displacement efficiency at elevated temperatures, *J. Dispers. Sci. Technol.* 36 (9) (2015) 1274–1281.
[28] J.F. Jin, Y.L. Wang, T.A.H. Nguyen, A.V. Nguyen, M.Z. Wei, B.J. Bai, The effect of gas-wetting nano-particle on the fluid flowing behavior in porous media, *Fuel* 196 (2017) 431–441.
[29] N. Pal, A. Mandal, Numerical simulation of enhanced oil recovery studies for aqueous gemini surfactant-polymer-nanoparticle systems, *AIChE J.* 66 (11) (2020) 17020.
[30] G. Cheraghian, S.S. Khalili Nezhad, M. Kamari, M. Hemmati, M. Masihi, S. Bazgir, Effect of nanoclay on improved rheology properties of polyacrylamide solutions used in enhanced oil recovery, *J. Petroleum Explor. Prod. Technol.* 5 (2) (2015) 189–196.
[31] A. Steele, I.S. Bayer, E. Loth, Pipe flow drag reduction effects from carbon nanotube additives, *Carbon* 77 (2014) 1183–1186.
[32] M.L. Luo, X.D. Si, M.Z. Li, X.H. Jia, Y.L. Yang, Y.P. Zhan, Experimental study on the drag reduction performance of clear fracturing fluid using wormlike surfactant micelles and magnetic nanoparticles under a magnetic field, *Nanomaterials (Basel)* 11 (4) (2021) 885.
[33] M.E. Rosti, L. Brandt, Increase of turbulent drag by polymers in particle suspensions, *Phys. Rev. Fluids* 5 (4) (2020) 041301.
[34] S.M. Fotukian, M.N. Esfahany, Experimental study of turbulent convective heat transfer and pressure drop of dilute CuO/water nanofluid inside a circular tube, *Int. Commun. Heat Mass Transf.* 37 (2) (2010) 214–219.
[35] A. Moosaie, N. Shekouhi, N.M. Nouri, M. Manhart, An algebraic closure model for the DNS of turbulent drag reduction by Brownian microfiber additives in a channel flow, *J. Non Newton. Fluid Mech.* 226 (2015) 60–66.
[36] B. Raei, S.M. Peyghambarzadeh, R.S. Asl, Experimental investigation on heat transfer and flow resistance of drag-reducing alumina nanofluid in a fin-and-tube heat exchanger, *Appl. Therm. Eng.* 144 (2018) 926–936.
[37] G.D. Kalaycioglu, D. Yuksel, B. Okmen, N. Aydogan, Interfacial properties and aggregates of novel redox-active surfactant to synthesize silver nanoparticles at the air/water interface, *Colloids Surf. A Physicochem. Eng. Aspects* 624 (2021) 126759.
[38] A.R. Pouranfard, D. Mowla, F. Esmaeilzadeh, An experimental study of drag reduction by nanofluids through horizontal pipe turbulent flow of a Newtonian liquid, *J. Ind. Eng. Chem.* 20 (2) (2014) 633–637.
[39] J.B. Crews, A.M. Gomaa, Nanoparticle-associated surfactant micellar fluids: An alternative to crosslinked polymer systems, In: SPE International Oilfield Nanotechnology Conference, Noordwijk, Netherlands, 2012.
[40] S. Paryani, S.A.A. Ramazani, Investigation of the combination of TiO_2 nanoparticles and drag reducer polymer effects on the heat transfer and drag characteristics of nanofluids, *Can. J. Chem. Eng.* 96 (6) (2018) 1430–1440.
[41] J.D. Brassard, D.K. Sarkar, J. Perron, Studies of drag on the nanocomposite superhydrophobic surfaces, *Appl. Surf. Sci.* 324 (2015) 525–531.
[42] T. Sharma, J.S. Sangwai, Silica nanofluids in polyacrylamide with and without surfactant: Viscosity, surface tension, and interfacial tension with liquid paraffin, *J. Petroleum Sci. Eng.* 152 (2017) 575–585.
[43] L. Xing, Y.C. Ke, X. Hu, P. Liang, Preparation and solution properties of polyacrylamide-based silica nanocomposites for drag reduction application, *New J. Chem.* 44 (23) (2020) 9802–9812.
[44] A.S. Pereira, R.M. Andrade, E.J. Soares, Drag reduction induced by flexible and rigid molecules in a turbulent flow into a rotating cylindrical double gap device: Comparison between poly(ethylene oxide), polyacrylamide, and xanthan gum, *J. Non Newton. Fluid Mech.* 202 (2013) 72–87.
[45] T. Rodrigues, F.J. Galindo-Rosales, L. Campo-Deaño, Critical overlap concentration and intrinsic viscosity data of xanthan gum aqueous solutions in dimethyl sulfoxide, *Data Brief* 33 (2020) 106431.
[46] G. Xie, Y. Shen, A study on the rheological properties and viscoelasticity of PAM aqueous solutions, *J. Nat. Sci. Heilongjiang Univ.* 20 (4) (2003) 89–91. (in Chinese)
[47] A.R. Pouranfard, D. Mowla, F. Esmaeilzadeh, An experimental study of drag reduction by nanofluids in slug two-phase flow of air and water through horizontal pipes, *Chin. J. Chem. Eng.* 23 (3) (2015) 471–475.
[48] D.J. Liu, S. Wang, I. Ivitskiy, J.J. Wei, O.K.C. Tsui, F. Chen, Enhanced drag reduction performance by interactions of surfactants and polymers, *Chem. Eng. Sci.* 232 (2021) 116336.
[49] I. Sher, G. Hetsroni, A mechanistic model of turbulent drag reduction by additives, *Chem. Eng. Sci.* 63 (7) (2008) 1771–1778.
[50] S. Özerinç, S. Kakaç, A.G. Yazıcıoğlu, Enhanced thermal conductivity of nanofluids: A state-of-the-art review, *Microfluid. Nanofluid.* 8 (2) (2010) 145–170.
[51] Z.Y. Liu, F.J. Zhou, H.Y. Qu, Z. Yang, Y.S. Zou, D.B. Wang, Impact of the microstructure of polymer drag reducer on slick-water fracturing, *Geofluids* 2017 (2017) 9080325.
[52] Y. Rabin, B.J. Zielinska, Scale-dependent enhancement and damping of vorticity disturbances by polymers in elongational flow, *Phys. Rev. Lett.* 63 (5) (1989) 512–515.
[53] B. Toms, Some observations on the flow of linear polymer solutions through straight tubes at large Reynolds numbers, In: Proceedings of the First International Congress on Rheology, Amsterdam (1948).
[54] P.S. Virk, An elastic sublayer model for drag reduction by dilute solutions of linear macromolecules, *J. Fluid Mech.* 45 (3) (1971) 417–440.